Available online at www.sciencedirect.com
SCIENCE DIRECT
Polymer 47 (2006) 4318–4327
polymer
www.elsevier.com/locate/polymer

# Toughening of dimethacrylate resins by addition of ultra high molecular weight polyethylene (UHMWPE) particles

Rahul A. Ranade [a], Stephanie L. Wunder [a,*], George R. Baran [b]

[a] Department of Chemistry, Temple University, 1901 N 13th Street, Philadelphia, PA 19122, USA
[b] Department of Mechanical Engineering, Temple University, Philadelphia, PA 19122, USA

Received 22 December 2005; received in revised form 29 March 2006; accepted 1 April 2006

**Abstract**

The effects of the addition of UHMWPE particles, of nominal ⟨80 μm⟩ size, on the fracture toughness, flexural modulus and strength of composites made with dimethacrylate resins (60/40 wt/wt BisGMA–TEGMA) were investigated as a function of volume fraction of UHMWPE (0–60 vol%) and particle surface treatment. Interfacial shear strengths ($\tau$) were measured via microbond shear strength tests using Spectra900™ (UHMWPE) fibers and BisGMA–TEGMA beads. $\tau$ increased by a factor of 4 compared with untreated UHMWPE, and surface treated particles improved the mechanical properties of the composite. Fracture toughness ($K_{IC}$) and flexural modulus ($E$) increased with increased volume fraction of UHMWPE, with maximum $K_{IC}/E$ increases (at 60 vol%) of 238%/25% compared with the neat resin. SEM images showed debonding as well as yielding and fibrillation of the UHMWPE particles, suggesting that these were significant toughening mechanisms.


*Keywords:* UHMWPE; Composites; Toughening

## 1. Introduction

Dental composites and acrylic bone cements are typically prepared from brittle dimethacrylate resins that can fracture and wear. Fracture results both from the development of microscopic cracks originating in areas of stress concentration (flexural fatigue) or from the application of a sudden force (impact). Increase in fracture toughness without decrease in strength has been the goal of numerous research efforts to improve the performance of dental resin composites and acrylic bone cements. Some improvements in toughness have been achieved through modifications of the resin itself [1], for example formulations of polybutadiene/bis-phenol A copolymers [2], dimethacrylate resins with aromatic 'hard' segments and polybutadiene 'soft' segments [3], and Bis-phenol-A bis-(2-hydroxypropyl) methacrylate (BisGMA)/tri(ethylene glycol) dimethacrylate (TEGDMA) resins with methacrylate-terminated poly(butadiene-acrylonitrile-acrylic acid) terpolymers [4]. Another approach to improve fracture toughness has been to reduce areas of stress concentration by introducing sites for internal stress relief, through the incorporation of porosity [5].

The most common method for improvement of fracture toughness in brittle resins, such as those formed from dimethacrylates or polymethylmethacrylate (PMMA), is through the addition of fillers [6], which can be rubber [7–9], inorganic [10] or core–shell particles [1,9,11]. The mechanism or combinations of mechanisms through which energy is dissipated can be different depending on many factors such as the type, volume fraction, size and shape of filler, as well the degree of adhesion between the filler and matrix [12–14]. In general, rubber provides the largest toughening increase, but at the expense of a decrease in modulus of the composite, whereas inorganic particles provide less toughening, but with improvements in the modulus. In rubber-reinforced composites, toughening is believed to be the result of cavitation of the rubber particles followed by [15,16] or coupled with [17] shear yielding of the matrix. This is manifest by holes in fracture surfaces that are larger than the original rubber particles, and in the beveled edges of the voids [18]. In inorganic-reinforced composites (such as with glass spheres), toughening occurs through crack pinning, microcrack formation, debonding and shear yielding, although there is debate concerning interpretation of the microscopy images of the fracture surface [19,20]. The performance of glass-reinforced composites is also affected by the adhesion between the particles and the matrix

* Corresponding author. Tel.: +1 215 204 5046; fax: +1 215 205 1532.
*E-mail address:* slwunder@temple.edu (S.L. Wunder).

0032-3861/$ - see front matter © 2006 Published by Elsevier Ltd.
doi:10.1016/j.polymer.2006.04.004

[21–23], which is often improved through the use of compatible silane coupling agents [24].

High-density polyethylene (HDPE) [25] and ultra high molecular weight polyethylene (UHMWPE) fibers [26–33] and beads [34,35], and UHMWPE coated glass beads [36] have also been used as fillers to improve mechanical properties of acrylic dental-composites and bone cements due to their high toughness, chemical and abrasion resistance, and low moisture absorption. Since polyethylene is chemically inert, methods have been developed to increase the wettability or chemical bonding of the low surface energy filler with polar matrix resins. Surface modification techniques such as corona and plasma discharge [30,32,37] have been used to introduce high surface energy groups such as carbonyl, hydroxyl or carboxyl functionalities to PE or UHMWPE, which may then bond either physically or chemically to the resin [25,35,38,39]. Chromic acid grafting of functional silanes of UHMWPE (in the gel state) using peroxides [40], hydroperoxide-initiated grafting of polymers [41], chemical oxidation polymerization [42] onto UHMWPE fibers and swelling/chemical methods [43], have been used to improve adhesion to resins.

The goal of the current work was to investigate the use of UHMWPE powder as filler for BisGMA–TEGDMA based dental composites to improve fracture toughness without significant loss in other mechanical properties, and to use SEM to elucidate the toughening mechanism. The UHMWPE powder was used as received, or with surface treatments designed to enhance wetting or chemical bonding of the UHMWPE to the polar BisGMA/TEGDMA resin. The bonding between the UHMWPE surface and resin matrix was evaluated by surface treatment of Spectra900™ fibers (Honeywell, Inc.) and measurement of the interfacial strength ($\tau$) by microbond shear tests, which was developed for small diameter fibers [44–46], and for which the stress distribution is similar to that in a real brittle matrix composite. Only the apparent interfacial shear strength values, which are average values, were reported, and thus only qualitative differences between the efficiency of the surface modifications were obtained. More quantitative characterization of the data, in which local interfacial parameters instead of the average values are used, which takes into account the contributions of both bonding and friction to adhesion [47,48] and which includes the effect of bead geometry on the stresses [49], permits better correlation with molecular parameters.

Composites were made at 0, 5, 10, 20, 25, 30 and 60 filler volume percent without surface treatment and with surface treatments that provided wetting/covalent bonding to the resin. The effect of the UHMWPE filler on the fracture toughness, flexural modulus and flexural strength of the composites was evaluated. At 60% loading of treated UHMWPE particles, fracture toughness increased 230% compared with the neat resin but there was also a decrease of ~50% in the flexural strength. The moduli of all the composites increased up to about 25% compared with the neat resin. Significant debonding and rupture of the UHMWPE particles was observed on the fractures surfaces of the composites that failed in three-point bending.

## 2. Materials and methods

### 2.1. Chemicals

Spectra900™ fibers (1200 Denier), kindly provided by Honeywell Inc. were washed by refluxing with acetone at 56 °C for 2 h followed by overnight evacuation at room temperature (to remove the sizing). Bis-phenol-A bis-(2-hydroxypropyl)-methacrylate(BisGMA), tri(ethylene glycol)dimethacrylate (TEGDMA), hydroquinone monomethylether (HMME), tertiary amine dimethylaminoethyl methacrylate (DMAEMA), polymethylmethacrylate (PMMA) and camphorquinone (CQ) were obtained from ESSTECH, stored under refrigeration and used as received. UHMWPE powder (nominal size $\langle 80\ \mu m \rangle$), *p*-xylene, decahydronapthalene (decalin), triethylamine (TEA) from Aldrich, 3-methacryloxypropyltrichlorosilane (Cl-MPS), octadecyltrimethoxy silane (M-OTS), and acetoxyethyltrichlorosilane (Cl-AES) were obtained from Gelest and used without further purification.

### 2.2. Preparation of the resin

0.06 kg of BisGMA were weighed into a Teflon beaker and mixed with 0.04 kg of TEGDMA (in the dark). This mixture was stirred manually with a glass rod until a uniform consistency was achieved. After addition of 0.0005 kg photosensitizer (CQ), 0.0005 kg reducing agent (DMAEMA) and 0.0000085 kg HQ, it was stirred overnight in the dark using a magnetic stirrer. The homogeneous mixture was then bottled and stored for future use.

### 2.3. Modification of UHMWPE surface

The surfaces of the Spectra900™ fibers/UHMWPE powder were modified using the coupling agents shown in Fig. 1. The following treatments, described below and shown in Scheme 1 were: (a) swelling with 5% octadecyltrimethoxy silane (M-OTS) solution in *p*-xylene at 110 °C for 2 h followed by quenching in dry ice (to prevent the diffusion of silane out of the UHMWPE) [50]; the reactions were carried out under $N_2$ purge, and the fibers/powder were rinsed/centrifuged in acetone and evacuated overnight at RT (vacuum 0.05 mmHg measured using a McLeod gauge).

The ethoxy/methoxy groups that were on or near the surface of all the fibers were then hydrolyzed in 0.1 M HCl for 30 min at 50 °C, followed by washing (3*x*) with acetone and overnight evacuation (0.05 mmHg) at RT. Lastly, the $-Si(OH)_3$ groups were reacted with Cl-MPS/Cl-AES, in order to attach methacrylate double bonds/polar groups that could react with/wet the resin. The fibers/powder were dispersed in anhydrous pentane and Cl-MPS/Cl-AES (25% by volume) was added using a preheated syringe; TEA was added as a catalyst. The reaction was carried out for 5 h at RT in an argon-purged glove box. The trichlorosilane end groups are expected to form a cross-linked silane layer on or below the fiber surface. The presence of TEA serves as a catalyst for enhanced silane attachment on silica surfaces, and thus might facilitate

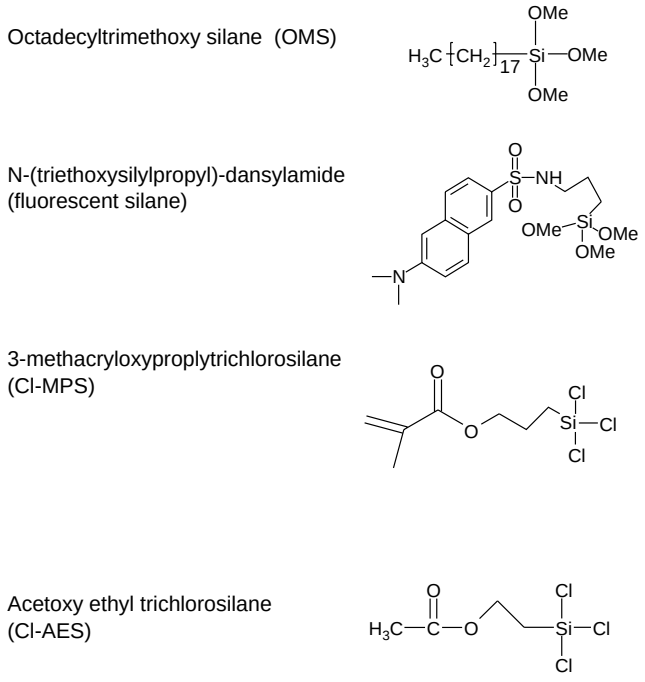


Fig. 1. Structures of silane coupling agents used for modification of UHMWPE fibers/particles.

crosslinking of the chlorosilane groups on the fiber surface as well. The Cl-MPS/Cl-AES treated fiber/powder was sonicated/centrifuged in pentane and methanol (3*x*) to remove the unattached free Cl-MPS/Cl-AES and TEA, respectively. The self-polymerized but unattached Cl-MPS floated or remained dissolved in both solvents and could be removed. The fibers/powder were evacuated (0.05 mmHg) at RT for 12 h.

### 2.4. Preparation of composites

Composites containing 5, 10, 20, 25, 30 and 60 vol% UHMWPE with or without surface treatment were prepared. The particles were dispersed into the resin (total volume 10 mL) manually using a glass rod, over a period of 2 h. After stirring, the mixture appeared visually homogeneous. Since the particles were over 80 μm in diameter and the resin was a clear liquid, a gradient in the refractive index could be observed when the particles eventually migrated towards the top of the resin. In order to avoid any demixing after homogeneity had been achieved, the composite mixture was immediately poured into a syringe, followed by injection and rapid cure (2 min) in the molds. SEM images of many samples showed that single particles and aggregates of up to four particles were typically observed.

### 2.5. Characterization

#### 2.5.1. Preparation of the microbond shear strength samples

The microbond shear strength samples were prepared by the spontaneous formation of fine resin beads on the fibers, as the dry fiber was pulled through a resin droplet. The beads were about 0.1–0.4 mm in embedded length and care was taken to ensure a spacing distance between them such that several specimens could be prepared along one fiber length. The fibers were cured in a light-curing oven (Dentsply/York division model TCU-II, 115 V, 600 W) for 4 min, and then placed in Petri dishes overnight at 37 °C. One end of the fiber was fixed onto a piece of cardboard using (5 min) epoxy, and allowed to completely cure overnight. The cardboard end of the sample was inserted in the top grip of an Instron tensile tester (Model 1122). The fixed bottom grip consisted of a specially made fixture [51] that had two glass slides that could be moved horizontally. The upper grip was used to position the bead just below the slides, which were closed until they just touched the outer surface of the fiber. The load was measured at a crosshead speed of 1 mm/min and testing was complete when the bead had been pulled from the fiber or the fiber failed.

The peak load from the load versus displacement curve was recorded and used to calculate the interfacial shear strength ($\tau$) from the following equation:

$$\tau = \left(\frac{F}{\pi d l}\right),$$

where $\tau$ is the apparent interfacial shear stress at failure, $F$ is the peak debonding load, $d$ is the fiber diameter and $l$ is the embedded length of the resin bead, which was measured using a microscope, and was in the range of 0.03–0.15 mm.

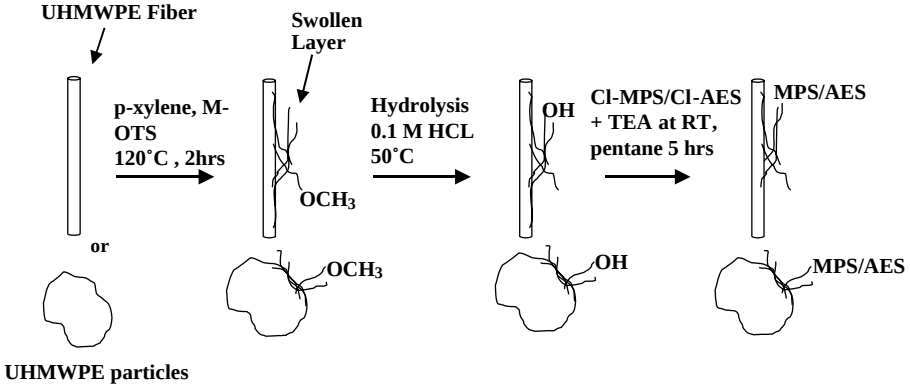


Scheme 1. Reaction showing surface modification of UHMWPE surface on fibers and particles.

*2.5.2. Flexural strength, flexural modulus and fracture toughness tests*

Flexural strength and flexural modulus of the composites were determined by a three-point bending test. Cross-sectional beams ($30\times2\times2$ mm$^3$) were prepared in a split steel mold, which had upper and lower (glass) cover plates. The sample bars were cured in a light-curing oven (Dentsply/York division model TCU-II, 115 V, 600 W) from the two opposite surfaces for 2 min. After curing, the samples bars ($n=10$) were removed from the mold and polished using 600 grit SiC paper. The polished samples were further cured at 37 °C in air for 12 h. The specimens were loaded to failure on a servo hydraulic tensile testing machine (MTS Mini-Bionix 2) at a crosshead speed of 1 mm/min. The distance between the support beams was 25 mm.

The flexural strength (in MPa) was calculated from the formula

$$\mathrm{FS} = \frac{3lF}{2BH^2}$$

where $l$ is the distance between the supports in mm, $F$ is the failure load ($N$), $B$ is the width and $H$ is the height of the beam in mm.

The flexural modulus (in GPa) was calculated from the formula:

$$E = \left(\frac{F}{D}\right)\left(\frac{l^3}{4BH^3}\right)$$

where $l$ is the distance between the supports in mm, $B$ and $H$ are the specimen width and height, respectively, in mm, and $F/D$ is the slope in the initial linear region of the load–displacement curve.

Bar-shaped, single-edge-notch bending, fracture toughness specimens (25 mm$\times$5.0 mm$\times$2.5 mm) were fabricated in a steel mold with a razor blade insert to produce a sharp notch at midspan ($a/W=0.5$), where $a$ = notch length and $W$ = specimen width. Fracture toughness ($K_{IC}$) was determined by single-edge notch beam method according to ASTM E399. Specimens ($25\times5\times2.5$ mm$^3$) were prepared in a steel mold with a razor blade insert to produce a sharp notch at midspan ($a/W=0.5$), where $a$ = notch length and $W$ = specimen width. Curing and storage conditions were similar to those described in the flexural strength test. The specimens were loaded to fracture at a crosshead speed of 0.1 mm/min.

$K_{IC}$ was calculated for each specimen according to the following formula

$$K_{IC} = \frac{P_f L f(a/W)}{BW^{1.5}}$$

where $P_f$ is the fracture load ($N$), $L$ is the span length in mm, $B$ is the thickness and $W$ is the width of the specimen in mm. $f(a/W)$ is a function of a and $W$ as described in ASTM E399. After the fracture toughness test, the fragments of the composite specimens were mounted on aluminum stubs and sputter coated for SEM evaluation (JEOL 6300FV).

## 3. Results

### 3.1. Microbond shear strengths

The results of the microbond shear strength tests are presented in Table 1, along with data for silica fibers (with or without MPS treatment) using BisGMA/TEGDMA beads. The interfacial strength increased about four-fold for BisGMA/TEGDMA beads on the UHMWPE fibers for the treated versus untreated fibers. For the samples in which OMS was subsequently reacted with Cl-MPS or Cl-AES, the former had slightly greater interfacial bonding. The values of $\tau$ ($\approx$4 MPa) for these surface treatment methods for UHMWPE were approximately the same as that obtained for untreated glass fibers. By contrast, for MPS treated glass fibers, a value of $\tau$ of 15.0 MPa was obtained.

### 3.2. Mechanical property data

The fracture toughness ($K_{IC}$), flexural modulus ($E$) and flexural strength ($\sigma$) data are presented in Figs. 2–4, and summarized in Table 2. Both fracture toughness and modulus increase upon addition of UHMWPE, but with a decrease in flexural strength. Fig. 2 shows that addition of increasing amounts of UHMWPE result in increased fracture toughness for the untreated, Cl-MPS and Cl-AES treatments, as expected based on the increased fracture toughness of UHMWPE compared with the BisGMA/TEGDMA resin. At a fixed volume percent of UHMWPE filler, fracture toughness increased in the order $K_{IC}$(Cl-AES) > $K_{IC}$(Cl-MPS) > $K_{IC}$ (untreated). A maximum toughness increase of 238% was observed at 60% loading of the Cl-AES treated UHMWPE.

Table 1
Interfacial shear strengths of BisGMA–TEGDMA (60/40) beads on surface treated Spectra900™ UHMWPE or *E*-glass fibers

| Fiber | Treatment | Interfacial strength (MPa) |
|---|---|---|
| UHMWPE | No treatment | 1.06 ($\pm$0.18) |
| UHMWPE | Swelling with fluorescent silane at 110 °C for 2 h followed by hydrolysis and Cl-MPS + TEA treatment | 4.09 ($\pm$0.75) |
| UHMWPE | Swelling with 5% OMS at 110 °C for 2 h followed by hydrolysis and Cl-MPS + TEA treatment | 4.22 ($\pm$0.28) |
| UHMWPE | Swelling with 5% PE-silane at 110 °C for 2 h followed by hydrolysis and Cl-MPS + TEA treatment | 2.98 ($\pm$0.41) |
| UHMWPE | Swelling with OMS at 110 °C for 2 h followed by hydrolysis and Cl-AES and TEA treatment | 3.89 ($\pm$0.29) |
| UHMWPE | Plasma treatment with $SiO_2$ + MPS | 4.01 ($\pm$0.52) |
| *E*-glass | No treatment | 3.77 ($\pm$0.50) |
| *E*-glass | MPS silanization | 15.05 ($\pm$1.71) |

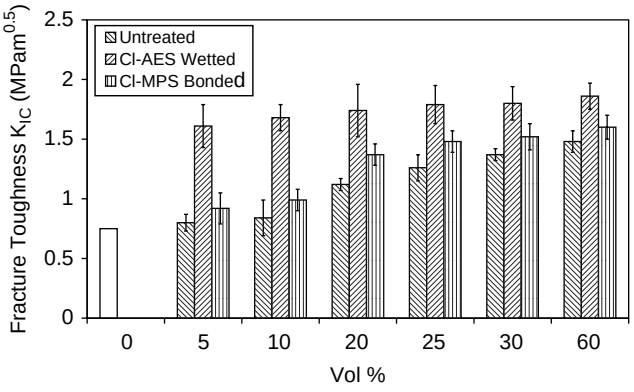


Fig. 2. Fracture toughness, $K_{IC}$ (MPam$^{1/2}$) as a function of volume percent UHMWPE for untreated, Cl-AES and Cl-MPS treated particles.

In the case of glass beads, fracture toughness is usually observed to increase with increase in volume fraction of beads, but the incremental toughening effect decreases with increasing volume fraction [52]. This same effect is observed for the addition of UHMWPE particles, especially for the Cl-MPS and untreated particles, where there is minimal change in $K_{IC}$ between 30 and 60 vol% UHMWPE. At 30 vol%, $K_{IC}$ for the UHMWPE/BisGMA/TEGDMA resins was twice as great as for the glass filled systems [53]. However, for the UHMWPE filled systems, $K_{IC}$ was very similar for 30 and 60 vol%, whereas $K_{IC}$ doubled between 30 and 60 vol% for the glass filled systems [53]. At 60 vol% the order of fracture toughness was $K_{IC}$(Cl-AES/UHMWPE) > $K_{IC}$(Cl-MPS/UHMWPE) ~ $K_{IC}$(MPS/glass) > $K_{IC}$(untreated/UHMWPE) > $K_{IC}$(untreated/glass). Thus, although treated UHMWPE always improved the fracture toughness of the BisGMA/TEGDMA resin up to 60 vol% loading, the incremental improvements were greatest below 30 vol%.

The data presented in Fig. 3 and Table 2 indicates that the improvements in toughness were not gained at the expense of a decrease in modulus, and in fact that there were increases of about 30% in the moduli of the composites (average of 3.7 GPa) compared with the neat resin (2.8 GPa). Although the UHMWPE surface treated with Cl-MPS, and thus capable of forming covalent bonds with the resin, had the highest values

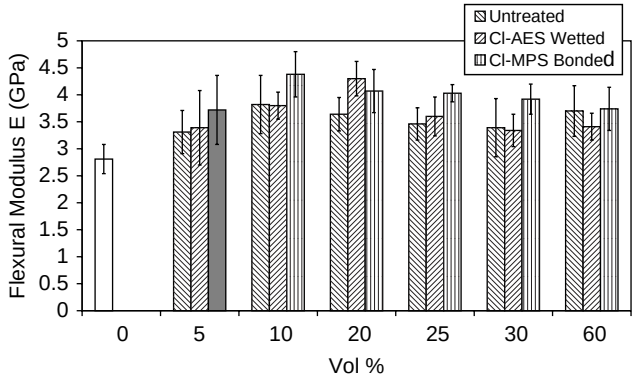


Fig. 3. Flexural modulus, $E$ (GPa) as a function of volume percent UHMWPE for untreated, Cl-AES and Cl-MPS treated particles.

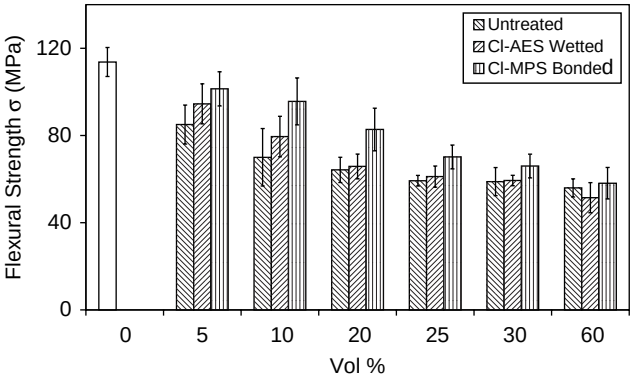


Fig. 4. Flexural strength, $\sigma$ (MPa) as a function of volume percent UHMWPE for untreated, Cl-AES and Cl-MPS treated particles.

of $E$ at all volume fractions (except 20 vol%) all the values were similar within experimental error).

In order to understand the increase in modulus of all the samples compared with the neat resin, it is useful to investigate the crystallinity of the UHMWPE particles used to make the composites. The modulus of UHMWPE depends considerably on processing conditions, varying from ~0.8 to 1.4 GPa for compression molded samples to 40–70 GPa when drawn, and it is difficult to measure the modulus of the ~80 μm irregularly shaped particles. However, the degree of crystallinity is higher for the 'as received' powder compared with compression molded samples, as shown in Fig. 5, where $\Delta H_m$ decreases from 190 to 120 J/g and $T_m$ decreases from 144 to 135 °C when the 'as received' powder is melted. These values are similar to those measured for UHMWPE molded sheets obtained commercially [54,55].

Fig. 4 shows the clear decrease in flexural strength with increasing volume percent of UHMWPE for the untreated, Cl-MPS and Cl-AES treatments. The flexural strength was

Table 2
Composite mechanical properties of UHMWPE filled BisGMA–TEGDMA (60/40) resins

| Filler type | Filler (vol%) | $E$ (GPa) | $\sigma$ (MPa) | $K_{IC}$ MPam$^{0.5}$ |
|---|---|---|---|---|
| None | 0 | 2.81 (0.27) | 113.7 (6.65) | 0.75 (0.05) |
| Untreated | 5 | 3.31 (0.40) | 85 (8.95) | 0.80 (0.07) |
| | 10 | 3.82 (0.54) | 70 (13.2) | 0.84 (0.15) |
| | 20 | 3.64 (0.31) | 64.21 (5.81) | 1.12 (0.05) |
| | 25 | 3.46 (0.30) | 59.25 (2.45) | 1.26 (0.11) |
| | 30 | 3.39 (0.54) | 58.85 (6.45) | 1.37 (0.05) |
| | 60 | 3.70 (0.47) | 55.95 (4.15) | 1.39 (0.09) |
| Cl-AES | 5 | 3.39 (0.69) | 94.50 (9.20) | 1.61 (0.18) |
| (wetted) | 10 | 3.80 (0.25) | 79.50 (9.3) | 1.68 (0.11) |
| | 20 | 4.30 (0.32) | 65.8 (5.70) | 1.74 (0.22) |
| | 25 | 3.60 (0.36) | 61.15 (4.85) | 1.79 (0.16) |
| | 30 | 3.34 (0.30) | 59.35 (2.4) | 1.80 (0.14) |
| | 60 | 3.21 (0.25) | 50.55 (6.90) | 1.82 (0.11) |
| Cl-MPS | 5 | 3.72 (0.64) | 101.4 (7.84) | 0.92 (0.13) |
| (bonded) | 10 | 4.38 (0.42) | 95.65 (10.75) | 0.99 (0.09) |
| | 20 | 4.07 (0.40) | 82.74 (9.76) | 1.37 (0.09) |
| | 25 | 4.03 (0.16) | 70.15 (5.45) | 1.48 (0.09) |
| | 30 | 3.92 (0.28) | 66 (5.45) | 1.52 (0.11) |
| | 60 | 3.82 (0.40) | 59.85 (7.25) | 1.59 (0.10) |

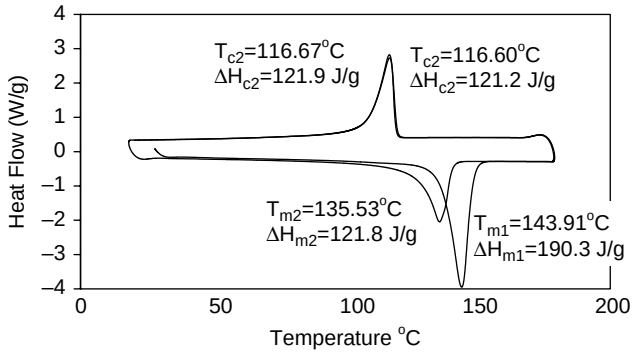


Fig. 5. DSC plot of as received UHMWPE powder, two heating and cooling cycles.

greatest for the UHMWPE treated with Cl-MPS and least for the composites prepared with the untreated UHMWPE.

### 3.3. SEM fracture surfaces

Typical SEM micrographs of the UHMWPE particles are shown in Fig. 6(A) and (B) at two magnifications. The irregular particles with rough surfaces have average dimensions of 80–100 μm × 100–150 μm. Fracture surfaces of 30 vol% UHMWPE in BisGMA/TEGDMA are presented in Fig. 7(A)–(D). There are several interesting features, which suggest the types of fracture modes that occur in these samples. The UHMWPE particles can be observed fractured, whole and still embedded in the matrix, and as the craters left by particle pull-out from the matrix. The average particle size of the craters left by the UHMWPE particles is the same as that of the original particles. The topography of these craters, as well as that of the particles left protruding from the resin is also the same as that of the original particles. There is no evidence of yielding of the resin near the particles, such as bent edges around the craters, as can be observed in rubber reinforced brittle matrices [18]. There is also no evidence of the tail structures observed in glass-reinforced composites, which are actually steps on the fracture surface that are formed when two secondary crack fronts divided by a glass bead meet with each other [52].

The most salient feature of the fracture surface is the propagation of the crack through the UHMWPE particles, producing what appears as yielding of the UHMWPE into many small fibrils from within the particle and microvoid formation. Occasionally, as observed at the bottom of Fig. 7(D), the result of the crack propagation was to pull out a portion of the UHMWPE particle in the form of a larger fibril; the static image does not convey that the pulled out portion was mobile on the fracture surface. By contrast, in rubber-reinforced composites, the rubber particles after rupture are believed to line the walls of the voids that are left behind [18].

Lastly, fracture through the resin produced the relatively smooth surface characteristic of brittle failure, as was also observed for the glass filled specimens [56], with additional step structures, sometimes occurring between two particles (or voids) and 'lance', also called 'river' or 'hackle' features.

All modes of fracture were observed for the untreated, Cl-AES and Cl-MPS treated beads. However, the greatest percentage of fracture through the UHMWPE particles occurred for the Cl-AES and Cl-MPS treatments, and the greatest number of pullout of UHMWPE particles without attached resin was observed for the untreated UHMWPE filled BisGMA/TEGDMA composites.

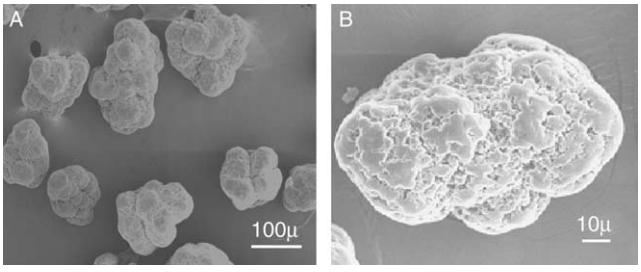


Fig. 6. SEM images of UHMWPE particles at two magnifications.

## 4. Discussion

The purpose of the current investigation was to determine whether addition of UHMWPE particles could improve the fracture toughness of a brittle, in this case BiSGMA–TEGDMA, resin without a concomitant loss in modulus, and further, to ascertain the toughening mechanism. Addition of UHMWPE did improve both the toughness and modulus of the composites, but with a decrease in flexural strength. Both surface treatments, namely attachment of Cl-AES, which was expected to improve the wettability of the UHMWPE to the polar BisGMA/TEGDMA resin, or Cl-MPS, which was expected to also enable bonding to the resin, increased $K_{IC}$ compared with untreated UHMWPE, but the effect was greater for the Cl-AES. In the case of the moduli, the data indicate that, within the experimental uncertainty, the untreated, Cl-AES and Cl-MPS treated samples had similar effects, that is, all the moduli increased by the same percentage with respect to the neat resin. Lastly, although the flexural strength decreased for all the samples compared with the neat resin, the decrease was least for the composites prepared with Cl-MPS, and was similar for the untreated and Cl-AES treated UHMWPE.

The results of the microbond shear strength data show that the effects of the Cl-AES and Cl-MPS treatments on UHMWPE are very similar to each other ($\tau \approx 4$ MPa), and significantly less than that obtained for surface treatment of glass fibers with MPS ($\tau \approx 15$ MPa). The similarity between the values of $\tau$ for BisGMA/TEGDMA beads on Cl-MPS/Cl-AES treated UHMWPE and untreated glass ($\tau \approx 4$ MPa) suggests that there are not many functional groups [Si–$CH_2$–$CH_2$–$CH_2$–O–C=O(C=$CH_2$–$CH_3$), Si–$CH_2$–$CH_2$–O–C=O($CH_3$)] on the surface of the UHMWPE after treatment, and that the product of the number and strength of the interactions are similar for the three surfaces. The slightly polar silica surface [containing SiOH groups] and the AES or MPS modified UHMWPE surface may have similar wetting affinity for the polar BisGMA/TEGDMA resin, resulting in similar values of $\tau$. For MPS treated silica, a monolayer (and sometimes multi-layers) of silane attaches to the surface, providing a higher

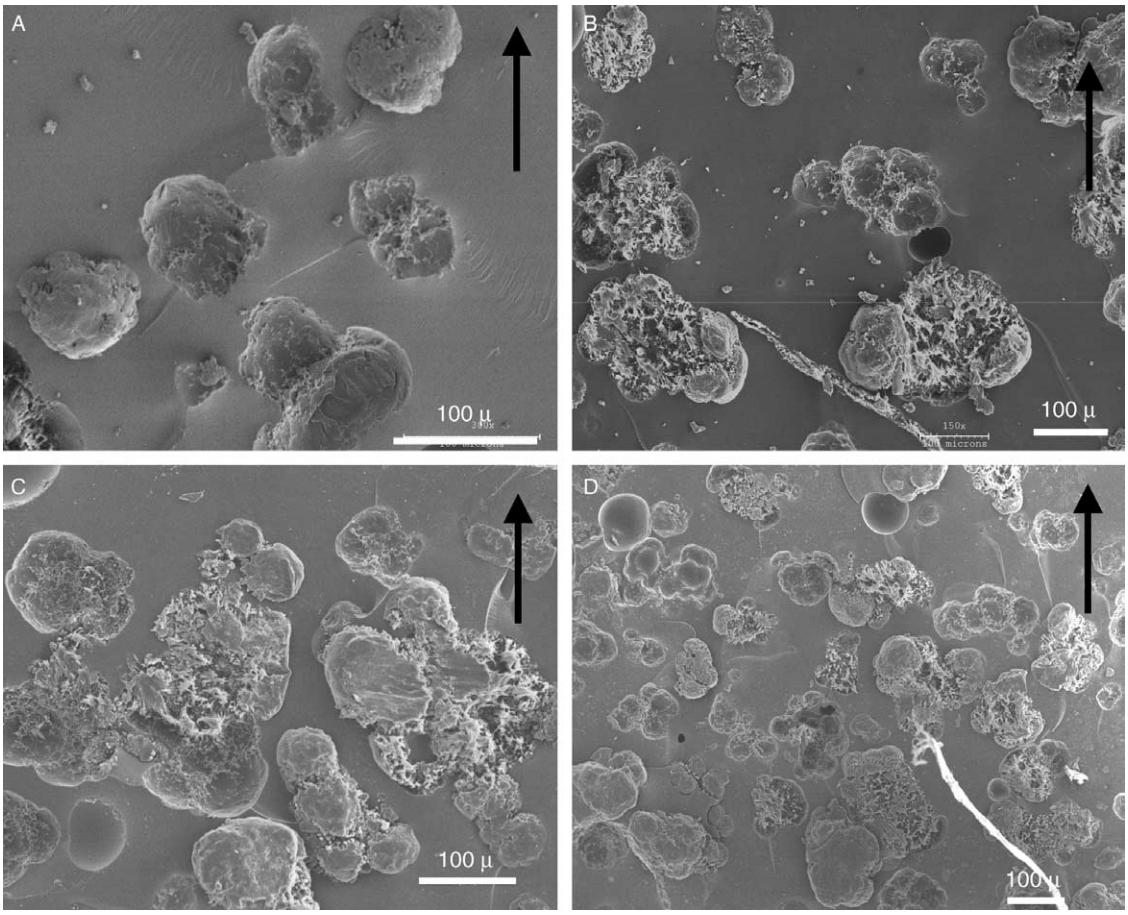


Fig. 7. SEM images of fracture surfaces of composites prepared with 30 vol% UHMWPE in BisGMA/TEGDMA (60/40) resin: (A) untreated; (B) Cl-AES treated; (C) Cl-MPS treated; (D) Cl-MPS treated at lower magnification showing large UHMWPE fibril. Arrows show direction of crack propagation.

density of reactive methacrylate sites [51]. Thus, it may be only for the MPS modified silica that significant covalent bonding with the resin takes place, although the slight increase in $\tau$ for the Cl-MPS compared with the Cl-AES treatment of UHMWPE may also reflect some covalent bonding for the former. The strength of the interfacial interactions, described by parameters such as interfacial shear stress ($\tau$), characterize load transfer through the interface. Only a more detailed analysis, which is beyond the scope of the current investigation, can correlate this data with the work of adhesion, which on a molecular level depends on the number and type of interfacial bonds [57–59].

Lastly, it should be pointed out that, unlike the smooth UHMWPE fibers used for the microbond shear tests, the treated UHMWPE particles are very irregular, so that mechanical interlocking of the resin with the particles may also contribute to the mechanical properties.

The improvement in toughening was expected, based on the higher toughness of UHMWPE compared with the brittle BisGMA/TEGDMA resin, and is consistent with other reports in the literature. Increases in fracture toughness have similarly been observed in acrylic resins reinforced with UHMWPE fibers [26] and chopped UHMWPE fibers [29]. However, no increases in fracture toughness were observed for untreated [34] or (proprietary) treated UHMWPE beads [35] up to 10% loading in acrylic resins. In the case of our untreated UHMWPE beads, there were also no significant increases in fracture toughness up to 10% loading compared with the neat resin. Thus, it is possible that the proprietary treatment on the UHMWPE particles [35] was not effective at compatibilizing the beads with the matrix.

Our data also suggests that the influence of the Cl-AES and Cl-MPS treatments on the toughness is similar, namely that they both increase the wetting of the UHMWPE particles to the resin, although, in addition, there may be a small amount of covalent attachment of the Cl-MPS treated UHMWPE to the resin. If this occurs, and it is easier for the Cl-AES treated UHMWPE to debond from the resin compared with the Cl-MPS treated UHMWPE, the contribution of debonding to the fracture toughness will be more important for the more easily debonded Cl-AES treated sample; the untreated UHMWPE, with no adhesion to the resin, would make no contribution via this mechanism to the fracture toughness.

Decreases in fracture toughness were previously observed when HDPE beads (untreated or with a reactive gas treatment) partially replaced glass in BisGMA/TEGDMA composites [25]. These results are also not in disagreement with our data. HDPE, which has lower fracture toughness than UHMWPE, was used in the study. More importantly, since both glass and HDPE act as impact modifiers, the results simply suggest that

at the concentration used in the study, glass was more effective than HDPE as an impact modifier.

Lastly, it should be pointed out that the intrinsic properties of UHMWPE particles are not easily measured, since the particles must first be fabricated (and thus subjected to some thermal treatment) into specimen shapes for testing. For neat polyethylene, a high volume fraction of amorphous material and low shear yield stress in the crystalline phase provide material toughness.

The increase in the moduli for all the UHMWPE filled composites was not sensitive to the surface treatment of the UHMWPE, suggesting that the improvements in moduli were not dependent on interfacial interactions between the components of the composite. Since, the moduli of the composites increased, the modulus of the UHMWPE was probably slightly greater than that of the neat resin; it was not possible to directly measure the modulus of individual 80 μm particles. The DSC data confirms that the crystallinity of the UHMWPE powder was greater than that for typical compression molded sheets (0.8–1.4 GPa), so that its modulus would also be slightly greater, and similar (but larger) in magnitude than that of the BisGMA/TEGDMA resin (2.8 GPa).

The behavior observed for the UHMWPE filler contrasts with that of glass-reinforced composites [$E$(glass) ~ 75 GPa], where there is a monotonic increase in modulus with volume fraction of glass, which is incrementally greater at higher volume fractions. For example, addition of glass beads resulted in moduli of BisGMA/TEGDMA composites that were twice (30 vol%) [36] or 4–5 times (60 vol%) as large as the neat resin [53]. The differences between the effects of glass versus UHMWPE may be attributed to the much greater mismatch in moduli with the resin in the former case. Even the simplest formula for addition of moduli cannot predict, within the experimental uncertainty of our measurements, a trend for two materials with moduli that differ by a factor of 2.

The moduli results for the UHMWPE reinforced composites are consistent with a previous investigation [34] in which addition of up to 7.5% UHMWPE powder resulted in ~20% increase in composite moduli (tested in water), followed by a decrease at 10% UHMWPE. Addition of UHMWPE fibers, which do have very high moduli, resulted in increases in moduli for some acrylic composites [26,29,33] and for others only when the fibers were grafted with methyl methacrylate [31]. Previous investigations have shown that partial replacement of glass filler with HDPE, which has a lower modulus than that of UHMWPE, resulted in a decrease in the modulus of composites prepared with bis-GMA/TEGDMA, an expected result since glass has a modulus significantly higher than either bis-GMA/TEGDMA or HDPE; comparisons with the neat resin were not included [25].

The decrease in flexural strength with increased volume fracture of filler is also expected. With increasing filler content there is a concomitant increase in surface area between the filler and the resin, providing additional sites at which failure can occur. It is interesting to note that the values of $\sigma$ at 30 and 60 vol% are close to (and slightly less than) the values for the untreated glass filler, and that these systems all had comparable values of $\tau$. This supports the idea that the interaction between the resin and either the untreated glass or treated UHMWPE particles results mostly from non-bonded polar interactions and relatively few covalent bonds, or that the product of the number and type of bonds are similar. By contrast, the values of $\sigma$ for the MPS treated glass beads, at 30 and 60 vol%, are nearly twice that for the UHMWPE (any treatment) particles. In these systems, in which there is a substantially higher value of $\tau$ (15 MPa), and considerable covalent bonding between the resin and filler, there are fewer additional sites for failure, resulting in higher values of $\sigma$.

The fact that the Cl-MPS treated UHMWPE has consistently higher (although not by a great amount) values of $\sigma$ than for the untreated or Cl-AES treated UHMWPE over the whole volume percent range, as well as slightly higher values of $\tau$ than for Cl-AES and a fourfold increase for untreated UHMWPE, suggests that the lack of bonding between the untreated and Cl-AES treated UHMWPE with the resin also provides increased numbers of sites for initiation of failure compared with the Cl-MPS treated UHMWPE, which may have a small number of covalent bonds with the resin. Our results are in agreement with previous investigations in which addition of UHMWPE powder resulted in the same or decreased strength of the composite materials [31,34,35,60], and in which fracture strengths of plasma treated PE fibers were greater than those of untreated fibers in PMMA resins [30].

SEM images can provide insight into what energy-dissipation processes are responsible for the enhancement in toughening in UHMWPE-filled glassy composites. The interesting feature about fracture in these composites is that some of the fracture occurred through the UHMWPE particles themselves. Previous studies of the fracture surfaces of composites prepared from acrylic resins and 10% untreated UHMWPE [34] or HDPE beads [25] showed similar impressions of the beads pulled from the resin, but no bead fracture. For the particles that did leave impressions after fracture, the average size of the craters was similar to the average particle size of the original particles. This suggests that some of the particles had debonded, and that the resin flowed around the particles before cure.

SEM images of BisGMA/TEGDMA resins reinforced with UHMWPE fibers have shown some fibers that have been extended [26], and very occasionally surface treated HDPE beads that were elongated [25], but not pulled out or ruptured. The fibrillar appearance for the fractured particles of UHMWPE is similar to that of fractured HDPE [61] and polycarbonate/polyethylene blends (PE is the matrix), where this morphology occurred at higher molding temperatures that resulted in increased crystallinity and more perfect crystals of the PE [62]. It was suggested that a rise in the crystallinity for high density PE decreased the brittle–ductile transition temperature and increased the fracture energy due to microvoid formation and the formation of fibrillar structures [61,63]. The UHMWPE particles in this work also have a relatively high percent crystallinity, compared with material that has been fabricated.

The similarity in the fracture surfaces despite surface treatment may be due to the relative ineffectiveness of the

surface treatments and to the irregularity of the particles themselves, which might result in mechanical bonding between the resin and the matrix. Adhesion improvement in polypyrrole treated UHMWPE fibers in an epoxy matrix was partially attributed to a surface roughening effect [42]. By comparison, SEM of fracture surfaces for glass filled BisGMA/TEGDMA composites showed predominantly fracture through the resin, for the treated silica, and particle pullout for the untreated silica, accompanied in both cases by the 'tails' characteristic of crack pinning [56].

## 5. Conclusions

Composites prepared from BisGMA–TEGDMA (60/40 wt/wt) resin were investigated in which ultrahigh molecular weight polyethylene (UHMWPE) powder, 0–60 vol% and ⟨80 μm⟩ in size, was used to improve fracture toughness without a loss in modulus. UHMWPE, which has high yield strength and modulus, but is non-polar and chemically inert, was used as is or modified to increase the wettability or reactivity with the resin matrix. Interfacial shear strength ($\tau$) between UHMWPE and the resin was measured via microbond shear strength tests using Spectra900™ (UHMWPE) fibers and BisGMA–TEGDMA beads. The surface of the fibers/powder was modified by simple swelling methods using octadecyltrimethoxy silane (Me-OTS), to allow diffusion of the reactive molecules into the UHMWPE surface; the trimethoxy groups were then hydrolyzed and reacted with either acetoxyethyltrichlorosilane (Cl-AES) or 3-methacryloxypropyltrichlorosilane (Cl-MPS), to provide groups that would either wet or react with, respectively, the methacrylate resin. Values of $\tau$ for $\tau$ (Cl-MPS)/$\tau$(Cl-AES) $\sim$ 4 MPa and were four times greater than $\tau$ (no treatment), compared with $\tau = 15$ MPa for MPS treated glass. In the case of the composite mechanical properties, fracture toughness ($K_{IC}$) improved with increased volume fraction of UHMWPE and in the order $K_{IC}$(Cl-AES, wet) > $K_{IC}$(Cl-MPS) > $K_{IC}$(untreated). The flexural modulus ($E$) increased from 2.8 GPa for the neat resin to between 3.2 and 4.4 GPa for the filled systems, and was relatively insensitive to either volume fraction of UHMWPE or to type of surface treatment of the UHMWPE. The flexural strength ($\sigma$) decreased with increasing volume fraction of UHMWPE, and increased in the order $\sigma$(Cl-MPS) > $\sigma$(Cl-AES) > $\sigma$(no treatment), suggesting that flaws at the interface resulted in failure. SEM images showed that significant debonding of UHMWPE from the resin occurred. In addition, there was fracture through the UHMWPE particles that resulted in microvoid formation and fibrillation of the particles. These were suggested to be major toughening mechanisms in the composites.

## Acknowledgements

We gratefully acknowledge NIH DE09530 for financial support and ESSTECH for donation of chemicals used in this work.

## References

[1] Cook WD, Forrest M, Goodwin A. Effect of resin structure and core–shell reinforcement on the yielding and fracture behavior of dental resins and their composites. Polym Prepr 2004;45:331–2.
[2] Teshima H, Matsukawa S. A study on the improvement of denture base resin. Epoxy dimethacrylate–polybutadiene dimethacrylate–MMA monomers as the liquid of denture base resin. Shika Zairyo Kikai 1990;9:509–19.
[3] Matsukawa S, Hayakawa T, Nemoto K. Development of high-toughness resin for dental applications. Dent Mater 1994;10:343–6.
[4] Kerby RE, Tiba A, Knobloch LA, Schricher SR, Tiba O. Fracture toughness of modified dental resin systems. J Oral Rehab 2003;30:780–4.
[5] Alster D, Feilzer AJ, Gee AJD, Mol A, Davidson CL. The dependence of shrinkage stress reduction on porosity concentration in thin resin layers. J Dent Res 1992;71:1619–22.
[6] Ferracane JL, Antonio RC, Matsumoto H. Variables affecting the fracture toughness of dental composites. J Dent Res 1987;66:1140–5.
[7] Rodford RA. Further development and evaluation of high impact strength denture base materials. J Dent 1990;18:151–7.
[8] Rodford RA, Braden M. Further observations on high impact strength denture-base materials. Biomaterials 1992;13:726–8.
[9] Hill RG. The role of microstructure on the fracture toughness and fracture behavior of rubber-reinforced acrylics. J Mater Sci 1994;29:3062–70.
[10] Rothon R. In: Rothon R, editor. Particle-filled polymer composites. New York: Longman; 1995.
[11] Perek J, Pilliar RM. Fracture toughness of composite acrylic bone cements. J Mater Sci, Mater Med 1992;3:333–44.
[12] Nielsen LE, Landel RF. Mechanical properties of polymers and composites. 2nd ed. New York: Marcel Dekker; 1994.
[13] Ahmed S, Jones FR. A review of particulate reinforcement theories for polymer composites. J Mater Sci 1990;25:4933–42.
[14] Michler GH, Bucknall CB. New toughening mechanisms in rubber modified polymers. Plast Rubber Compos 2001;30:110–5.
[15] Yee AF, Pearson RA. Toughening mechanisms in elastomer-modified epoxies. Part 1: mechanical studies. J Mater Sci 1986;21:2462–74.
[16] Wu J, Mai Y-W. Fracture toughness and fracture mechanisms of PBT/PC/IM blend. J Mater Sci 1993;28:6167–77.
[17] Chen X-H, Mai Y-W. Micromechanics of rubber-toughened polymers. J Mater Sci 1998;33:3529–39.
[18] Pearson RA, Yee AF. Toughening mechanisms in elastomer-modified epoxies. J Mater Sci 1986;21:2475–88.
[19] Lee J, Yee AF. Inorganic particle toughening I: micro-mechanical deformations in the fracture of glass bead filled epoxies. Polymer 2001;42:577–88.
[20] Kawaguchi T, Pearson RA. The moisture effect on the fatigue crack growth of glass particle and fiber reinforced epoxies with strong and weak bonding conditions. Compos Sci Technol 2004;64:1991–2007.
[21] Kawaguchi T, Pearson RA. The effect of particle-matrix adhesion on the mechanical behavior of glass filled epoxies. Part 1. A study on yield behavior and cohesive strength. Polymer 2003;44:4229–38.
[22] Kawaguchi T, Pearson RA. The effect of particle-matrix adhesion on the mechanical behavior of glass filled epoxies. Part 2. A study on fracture toughness. Polymer 2003;44:4239–47.
[23] Thio YS, Argon AS, Cohen RE. Role of interfacial adhesion strength on toughening polypropylene with rigid particles. Polymer 2004;45:3139–47.
[24] Mittal KL. Silanes and other coupling agents, vol. 2. Utrecht: Ridderkerk; 2000.
[25] Ferracane JL, Ferracane LL, Braga RR. Effect of admixed high-density polyethylene (HDPE) spheres on contraction stress and properties of experimental composites. J Biomed Res, Part B: Appl Biomater 2003;66B:318–23.
[26] Davy KWM, Parker S, Braden M, Ward IM, Ladizesky H. Reinforcement of polymers of 2,2 bis-4[2-htdroxy-3-methacryloyl propoxy] phenyl propane by ultra-high modulus polyethylene fibres. Biomaterials 1992;13:17–19.

[27] Braden M, Davy KWM, Parker S, Ladizesky NH, Ward IM. Denture base poly(methyl methacrylate) reinforced with ultra-high modulus polyethylene fibres. Br Dent J 1988;164:113–20.
[28] Gutteridge DL. The effect of including ultra high modulus polyethylene fibre on the impact strength of acrylic resin. Br Dent J 1988;164:177–80.
[29] Ladizesky NH, Cheng YY, Chow TW, Ward IM. Acrylic resin reinforced with chopped high performance polyethylene fiber-properties and denture construction. Dent Mater 1993;9:128–35.
[30] Ramos VJ, Runyan DA, Christensen LC. The effect of plasma-treated polyethylene fiber on the fracture strength of polymethyl methacrylate. J Prosth Dent 1996;76:94–6.
[31] Yang J-M, Huang P-Y, Yang M-C, Lo SK. Effect of MMA-*g*-UHMWPE grafted fiber on mechanical properties of acrylic bone cement. J Biomed Mater Res (Appl Biomater) 1997;38:361–9.
[32] Samadzadeh A, Kugel G, Hurley E, Aboushala A. Fracture strengths of provisional restorations reinforced with plasma-treated woven polyethylene fiber. J Prosth Dent 1997;78:447–50.
[33] Ellakwa AE, Shortall AC, Shehata MK, Marquis PM. The influence of fibre placement and position on the efficiency of reinforcement of fibre reinforced composite bridgework. J Oral Rehab 2001;28:785–92.
[34] Carlos NB, Harrison A. The effect of untreated UHMWPE beads on some properties of acrylic resin denture base material. J Dent 1997;25:59–64.
[35] Harrison A, Constantinidis VI, Vowles R. The effect of surface treated UHMWPE beads on some properties of acrylic resin denture base material. Eur J Prosthodont Restor Dent 1997;5:39–42.
[36] Ranade RA, Ding J, Wunder SL, Baran GR. Composites Part A: Applied Science and Manufacturing, In Press, Corrected proof available online 15 February 2006.
[37] Favia P, Stendardo MV, d'Agnostino R. Plasma treatment of polyethylene in $NH_3$–$N_2$ RF glow discharges. Plasmas Polym 1996;1:93–4.
[38] George GA. In: Feast WJ, Munro HS, Richards RW, editors. Polymer surfaces and interfaces. New York: Wiley; 1993.
[39] Favia P, Palumbo F, d'Agostino R. Grafting of functional groups onto polyethylene be means of RF glow discharges as a first step to the immobilisation of biomolecules; 1996.
[40] Mascia L, Dhillon J, Harper JF. Adhesion enhancement of rubbery and ductile polyolefin coatings on glass fibers for epoxy composites and effects on failure mechanisms. J Appl Polym Sci 1993;47:487–598.
[41] Arnold JJ, Zamora MP, Batich CD, Brennan AB. Hydroperoxide-initiated grafting of poly(styrene-stat-acrylonitrile)onto ultra-high modulus polyethylene fibers. J Adhes Sci Technol 1997;11:1343–58.
[42] Chiu HT, Wang J-H. Dynamical mechanical properties of the chemical oxidation on UHMWPE fibers for improved adhesion to epoxy resin matrix. J Appl Polym Sci 1998;68:1387–95.
[43] Debnath S, Ranade R, Wunder SL, Baran GR, Zhang J, Fisher ER. J Appl Polym Sci 2005;96:1564–72.
[44] Miller B, Muri P, Rebenfeld L. A microbond method for determination of the shear strength of a fiber/resin interface. Compos Sci Technol 1987;28: 17–32.
[45] Gaur U, Miller B. Microbond method for determination of the shear strength of a fiber/resin interface: evaluation of experimental parameters. Compos Sci Technol 1989;34:35–51.
[46] Miller B, Gaur U, Hirt D. Measurement and mechanical aspects of the microbond pull-out technique for obtaining fiber/resin interfacial shear strength. Compos Sci Technol 1991;42:207–19.
[47] Scheer RJ, Nairn JA. A comparison of several fracture mechanics methods for measuring interfacial toughness with microbond tests. J Adhes 1995;53:45–68.
[48] Pisanova E, Zhandarov S, Mader E. How can adhesion be determined from micromechanical tests? Compos Part A 2001;32:425–34.
[49] Ash JT, Cross WM, Svalstad D, Kellar JJ, Kjerengtroen L. Finite element evaluation of the microbond test: meniscus effect, interphase region, and vise angle. Compos Sci Technol 2003;63:641–51.
[50] Ranade R, Wunder SL, Baran GR. Surface modification of UHMWPE for improved interfacial adhesion in silica/methacrylate composites. Polym Mater Sci Eng 2003;88:260.
[51] Debnath S, Wunder SL, McCool JI, Baran G. Silane treatment effects on glass/resin interfacial shear strengths. Dent Mater 2003;19:441–8.
[52] Lee J, Yee AF. Fracture of glass bead/epoxy composites: on micromechanical deformations. Polymer 2000;41:8363–73.
[53] Ranade R, Ding J, Wunder SL, Baran GR. Dent Mater; Submitted.
[54] Yarovoy YK, Baran G, Wunder SL, Wang R. Submicron-size particles of ultrahigh molecular weight polyethylene produced via non-solvent and temperature-induced crystallization. J Biomed Mater Res 2000;53: 152–60.
[55] Rudnik E, Dobkowski Z. Thermal degradation of UHMWPE. J Therm Anal 1997;49:471–5.
[56] Debnath S, et al. Interface effects on mechanical properties of particle-reinforced composites. Dent Mater 2004;20:677–86.
[57] Zhandarov S, Mader E. Characterization of fiber/matrix interface strength: applicability of different tests, approaches and parameters. Compos Sci Technol 2005;65:149–60.
[58] Ash JT, Cross WM, Svalstad D, Kellar JJ, Kjerengtroen L. Finite element evaluations of the microbond test: meniscus effect, interphase region and vise angle. Compos Sci Technol 2003;63:641–51.
[59] Young RJ, Huang Y-L, Gu X, Day RJ. Analysis of composite test methods using Raman spectroscopy. Plast Rubber Compos Process Appl 1995;23: 11–19.
[60] Yang DH, Yoon GH, Kim SH, Rhee JM, Khang G. Surface and chemical properties of surface-modified UHMWPE powder and mechanical and thermal properties of it impregnated PMMA bone cement. III: effect of various ratios of initiator/inhibitor on the surface modification of UHMWPE powder; 2005.
[61] Ravi S, Takahashi K. Toughening mechanisms in annealed high density polyethylene under impact. Polym Eng Sci 2002;42:2146–55.
[62] Li Z-M, Qian Z-Q, Yang M-B, Yang W, Xie B-H, Huang R. Polymer 2005;46:10466–77.
[63] Kitao K. A study of brittle–ductile transition in polyethylene. Polym Eng Sci 1997;37:777–88.